



Identifying Areas Exposed to Potential Flash Floods and Drawing Map for Them Using Multi-Criteria Decision-Making Depending on GIS and AHP for Erbil Sub-Basin, Northern Iraq

Jumaa K. Mohammad Al – Shwani ^{1*} , Sabbar A. Saleh ² , Diary A. Mohammed Amin Al-Manmi ³ 

^{1,2}Applied Geological Department, College of Science, University of Tikrit, Tikrit, Iraq.

³Department of Petroleum and Energy Engineering, Technical College of Engineering, Sulaimani Polytechnic University, Sulaymaniyah, Iraq.

Article information

Received: 05- Jan -2024

Revised: 07- Mar -2024

Accepted: 01- Apr -2024

Available online: 01- Apr – 2025

Keywords:

Flash floods

AHP

GIS

Erbil City

Northern Iraq

ABSTRACT

Flash flooding is among natural calamities that cause a great deal of harm, including major economic losses, social unrest, and considerable infrastructure destruction worldwide and in Iraq specifically. Erbil basin is among the most susceptible areas in Iraq to torrents hazards, and although identifying and mapping flash flood-prone areas is a critical task for locals and those who make decisions to lower and manage the risk of flash floods, the aim of this research is to locate and map areas in Erbil, northern Iraq, that were vulnerable to flash floods by combining a GIS with an MCDM approach and (AHP). Flash flood-control factors such as elevation, slope, flow accumulation, rainfall, distance to rivers, drainage density, net runoff, land use land cover, groundwater depth, Normalized Difference Vegetation Index and soil types are combined, layered, and weighted to fulfill the study's purpose. According to the results, 23.36% of the basin has low to very low flooding susceptibility, and roughly 76.64% of basin has moderate to very high flooding susceptibility. It is discovered that the southwest and south of the research region, which is distinguished by low slope and elevation, high drainage density, flow accumulation, and land cover and land use, are more vulnerable to flood dangers. Final map of flood susceptibility, which is produced as a result of model's coherence with the recorded historical flood occurrences in study basin, demonstrated effectiveness of method used in the research to identify and map places vulnerable to flooding.

Correspondence:

Name: Jumaa K. Mohamad

Email: jumaageology22@gmail.com

DOI: [10.33899/earth.2024.145160.1188](https://doi.org/10.33899/earth.2024.145160.1188), ©Authors, 2025, College of Science, University of Mosul.

This is an open access article under the CC BY 4.0 license (<http://creativecommons.org/licenses/by/4.0/>).

تحديد المناطق المعرضة للفيضانات المفاجئة المحتملة ورسم خريطة لها باستخدام قرار متعدد المعايير يعتمد على نظم المعلومات الجغرافية و AHP لحوض أربيل الفرعي، شمالي العراق

جمعة كريم محمد الشواني^{1*} ID، صبار عبدالله صالح² ID، دياري علي محمد أمين³ ID

^{1,2} قسم علوم الأرض التطبيقية، كلية العلوم، جامعة تكريت، تكريت، العراق.

³ قسم هندسة النفط والطاقة، الكلية التقنية الهندسية، جامعة السليمانية، السليمانية، العراق.

الملخص

معلومات الأرشفة

تعد الفيضانات المفاجئة من بين الكوارث الطبيعية التي تسبب قدرًا كبيرًا من الضرر، بما في ذلك الخسائر الاقتصادية الكبيرة والمشاكل الاجتماعية والدمار الكبير للبنية التحتية في جميع أنحاء العالم وفي العراق على وجه التحديد. يعد حوض أربيل من بين أكثر المناطق عرضة في العراق لمخاطر السيول، وعلى الرغم من أن تحديد المناطق المعرضة للفيضانات ورسم خرائط لها يعد مهمة بالغة الأهمية للسكان المحليين وأصحاب القرار في الحكومة المحلية لتقليل مخاطر السيول وإدارتها، فإن الهدف من هذا البحث هو تحديد ورسم خريطة للمناطق المعرضة لمخاطر السيول والفيضانات في أربيل، شمالي العراق، التي كانت عرضة للفيضانات المفاجئة من خلال الجمع بين نظم المعلومات الجغرافية (GIS) ونهج تحليل القرار متعدد المعايير (MCDM) وعملية التسلسل الهرمي التحليلي (AHP). تم الجمع بين عوامل المؤثرة في الفيضانات المفاجئة مثل الارتفاع، والانحدار، وتراكم التدفق، هطول الأمطار السنوي، والمسافة من الأنهار، وكثافة الصرف، وصافي الجريان السطحي، واستخدام الأراضي والغطاء الأرضي، وعمق المياه الجوفية، ومؤشر الفرق الطبيعي للغطاء النباتي، ونوع التربة، الطبقات والمرجحة لتحقيق غرض الدراسة. وفقًا للنتائج، فإن 23.36% من الحوض لديه قابلية منخفضة إلى منخفضة للغاية للفيضانات، وحوالي 76.64% من الحوض لديه قابلية متوسطة إلى عالية للغاية للفيضانات. وقد تبين أن الجنوب الغربي والجنوب من منطقة البحث، والتي تتميز بانخفاض الانحدار والارتفاع، وارتفاع كثافة الصرف، وتراكم التدفق، والغطاء الأرضي واستخدام الأراضي، هي الأكثر عرضة لمخاطر الفيضانات. وأظهرت الخريطة النهائية لقابلية الفيضانات، والتي تم إنتاجها مع حوادث الفيضانات التاريخية المسجلة في منطقة الدراسة، فعالية الطريقة المستخدمة في البحث لتحديد ورسم خريطة للأماكن المعرضة للفيضانات.

تاريخ الاستلام: 05-يناير-2024

تاريخ المراجعة: 07-مارس-2024

تاريخ القبول: 01-ابريل-2024

تاريخ النشر الإلكتروني: 01-ابريل-2025

الكلمات المفتاحية:

السيول
AHP
GIS
مدينة أربيل
شمالي العراق

المراسلة:

الاسم: جمعة كريم محمد

Email: jumaageology22@gmail.com

DOI: [10.3389/earth.2024.145160.1188](https://doi.org/10.3389/earth.2024.145160.1188), ©Authors, 2025, College of Science, University of Mosul.

This is an open access article under the CC BY 4.0 license (<http://creativecommons.org/licenses/by/4.0/>).

Introduction

There is a sort of natural disaster known as the flash flood that is responsible for the most substantial amount of structural damage, major economic losses, and social unrest over the entire planet. The following sources have been cited: (Das and Gupta, 2021; Farhadi and Najafzadeh, 2021; Dang and Kumar, 2017; Hong, et. al., 2018 a, b). Flood damage has recently increased in many countries throughout the world as a result of climate change and environmental degradation brought on by incorrect land use management (Hagos et. al., 2022; Das and Gupta, 2021; Kanani-Sadat et. al., 2019; Ozkan. and Tarhan, 2016). Improper land use management contributes to both environmental deterioration and climate change. Flash

floods are one of the main natural disasters that affect people's lives, means of subsistence, and property in various parts of Iraq. Mapping and identifying flood-prone areas in Erbil district is the goal of this research. Although the district is known to be at risk of flooding in northern Iraq, no prior research has been done to locate and map flash flood-prone locations in it. For flood risk to be managed sustainably, it is necessary to comprehend risk and likelihood of flood episodes. (Binns, 2022). Potential mapping of flood risk areas is now seen as an important strategic tool for controlling, lowering, and mitigating the possible effects of flood risks. This is because maps can give people and stakeholders information about areas that might be prone to flooding (Abdelkarim *et.al.*, 2020) and (Rahmati *et.al.*, 2015). Past researchers have created several models and ways to study and map flood threats (Thannoun and Ismaeel, 2024). In recent times, most widely used method for assessing flood risks has the combined application of geospatial technologies. Multi-criteria decision analysis using the (AHP), (Allafta and Opp, 2021; Ajibade *et.al.*, 2021; Aydin and Birincioğlu, 2022; Karymbalis *et.al.*, 2021; Das and Gupta, 2021; Wubalem *et.al.*, 2021), frequency ratio (FR) (Wubalem *et.al.*, 2021; Ali *et.al.*,2020; Yariyan *et.al.*,2020; Tehrany *et.al.*,2017), hydrologic engineering centers, river analysis system (HEC-RAS) (Demir and Kisi, 2016), fuzzy logic (Kanani-Sadat *et.al.*,2019; (Ajibade *et.al.*,2021), logistic regression (LR) (Wubalem *et.al.*,2021; Ali *et.al.*,2020; Tehrany *et.al.*,2017), artificial neural networks (ANN) (Tamiru and Dinka, 2021), fuzzy weights of evidence (fuzzy-WofE) (Tehrany *et.al.*,2017; Hong, *et.al.*,2018a, b), support vector machine (SVM) (Son, *et.al.*,2021), random forest (RF) (Farhadi and Najafzadeh, 2021; Son et al., 2021; Zhao *et.al.*,2018; Wang *et.al.*,2015), two-dimensional flood routing model (FLO-2D) (Erena *et.al.*,2018) and the adaptive neuro-fuzzy inference system (ANFIS) The invaluable techniques developed and used by earlier researchers for mapping and identifying flood hazard areas are (Razavi-Termeh *et.al.*,2018; Hong *et.al.*,2018a, b); integrated with geographical technology (GIS and remote sensing). Several recent studies have mapped and located flood-prone areas using a combination of (MCDM) and (AHP) based on (GIS); for example, Abdelkarim *et.al.*, (2020) used the (AHP) along with GIS-based multi-criteria decision analysis to find out where in Al Shamal Train Pathway in Al Qurayyat area, Saudi Arabia, there is a high risk of flooding. The technique typically utilized in (MCDM) is the analytical hierarchy process (Abdelkarim et al., 2020). The technique has gained recognition for its exceptional ability to evaluate intricate decision-making tasks that frequently entail disparate data or standards, such as the mapping and identification of regions susceptible to flooding based on several parameters (Abdelkarim, *et.al.*,2020; Ali, *et.al.*,2020). This research aim is to identify and delineate flood-prone by utilizing a combination for GIS-based multi-criteria decision-making and (AHP) in Erbil sub-basin using eleven variables that have affected the likelihood of floods.

Study area

The research area is located in northern Iraq between 35°30'00" and 36°30'00" N and 43°30'00" and 44°30'00" E (Fig. 1). The area occupies 2107 Km². Elevations vary from 206 to 1076 meters above sea level. (Fig. 2). It is bordered from the northeast to the southwest by Kirkuk borders. The northeast of the area of interest frequently consists of hilly and mountainous areas, and the southwest is largely flat. A moderate slope makes up three-quarters of the research area, with the remaining quarter lying in the northeast and featuring modest anti-mass folds with overlapping decaying valleys.

According to the Erbil Meteorological Station, the climate of the study area is classified as semi-dry (Khoshnaw, 2022). The rainfall occurs between October and May and approximately disappears in months for June, July, August, and September; the highest average rainfall occurs in January (94 mm), and the average annual precipitation is 472.2 mm from 1992 to 2022.

Geologically, according to the Jassim and Goff, (2006), the exposed rocks in the area of interest belong to the Miocene, Middle Miocene, and Pliocene, which are of the Injana, Bai

Hassan, and Mukdadiyah formations. These rocks are buried under thick beds of Pleistocene and Holocene rocks (Fig. 3). The lithology of the Injana Formation is variable, but the unit is essentially composed of mostly red or grey-colored silty marl or claystones and siltstones of the same color, while the Bai Hassan Formation consists of an alternation of claystones and conglomerates with some sandstones and siltstones. The Mukdadiya Formation comprises up to 2000 m of fining upward cycles of gravely sandstone, red mudstone, and sandstone.

The major units of the Quaternary deposits involve the alluvial fan, depression fill, floodplain, and aeolian sediments. Quaternary sediments are unconsolidated, and their grains are finer than those of the underlying Mukdadiya and Bai Hassan Formations.

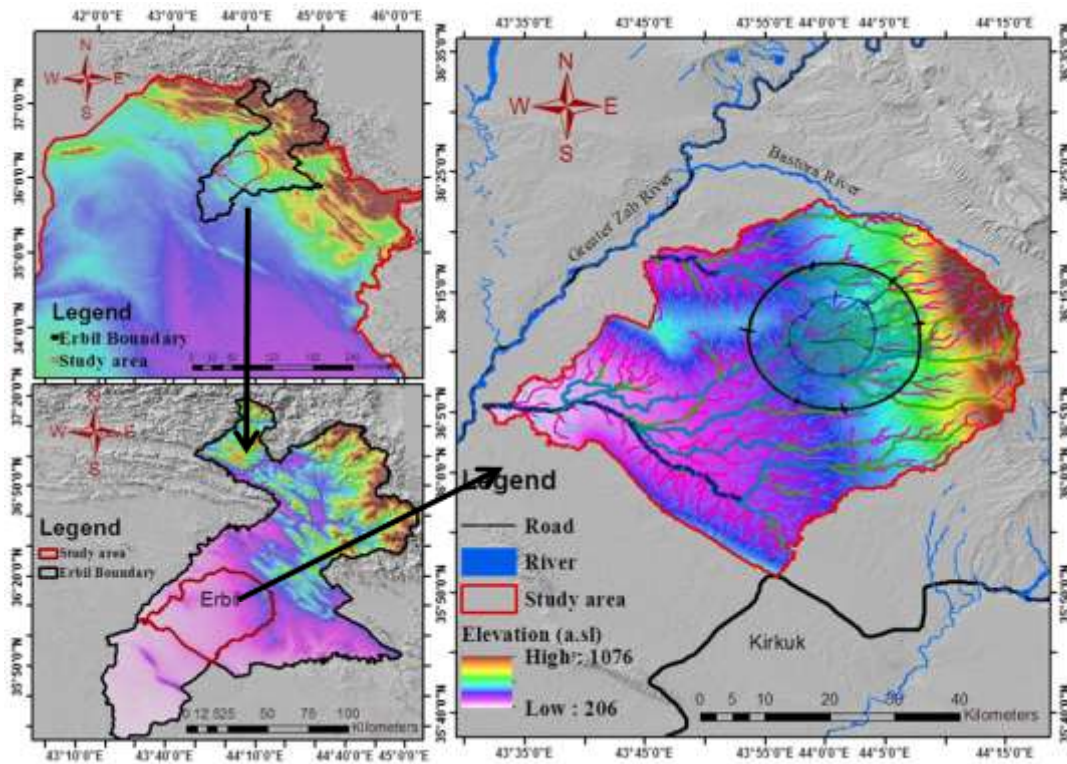


Fig. 1. Location map of Erbil Sub-basin

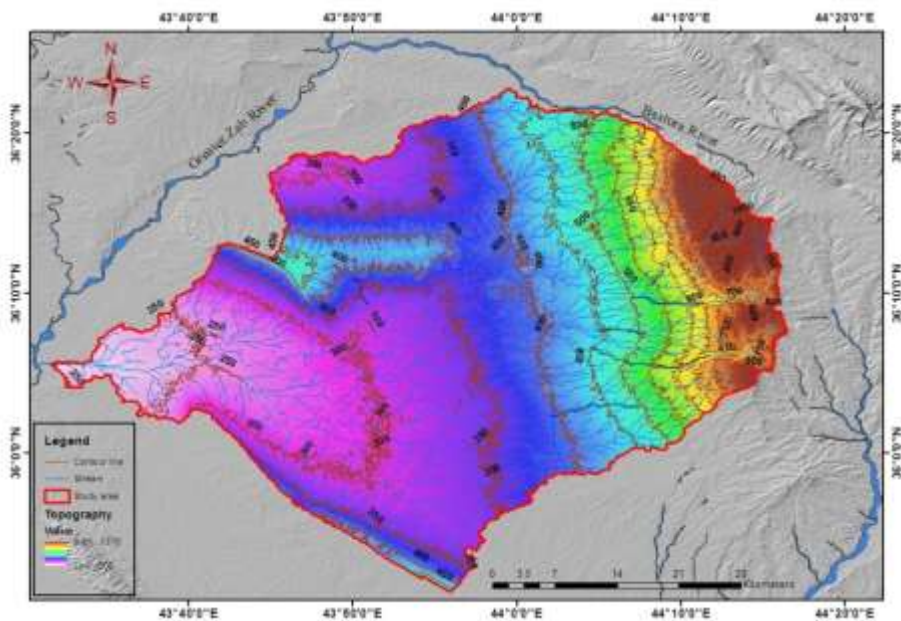


Fig. 2. Topographic map of Erbil Sub-basin

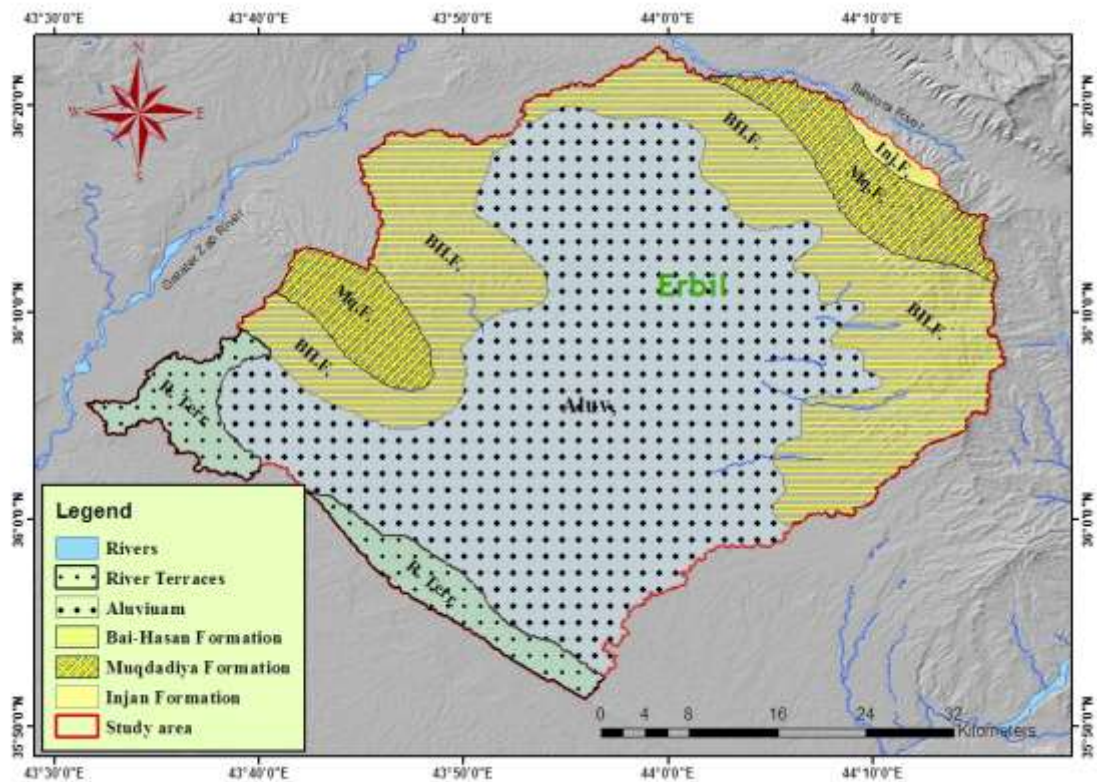


Fig. 3. Geological map of Erbil Sub-basin (Adopted from Jassim and Goff, 2006)

Materials and Methods

The necessary information for this investigation is gathered from several sources (Table 1). To retrieve several flood-controlling elements, the spatial resolution of the digital elevation model (STRM GDEM) is 12.5 m obtained from the US Geological Survey website. Additionally, a 10-meter spatial resolution Sentinel 2A satellite image (Band 4 and Band 5) obtained on March 27, 2022, is retrieved from the US Geological Survey website. Rainfall data (1992–2022) are gathered from the Erbil Meteorological Station from five meteorological stations which are (Benaslwa, Ankawa, Shamamik, Khabat, and Dewan). The depth of groundwater is measured for 115 wells distributed completely in the area of interest.

Table 1: Data sources and kinds used to map regions at risk of flooding

Data types	Data Sources
ASTER DEM Digital Elevation Model (12.5 m spatial resolution)	Downloaded from U.S Geologic Survey (http:// earth explo rer. usgs. gov/)
Sentinel 2 10 m spatial resolution Land Use/Land Cover (LULC) Map (2022)	Environmental System Research Institute (ESRI) (https:// livin gatlas.arcgis. com/ landc over/)
Monthly Rainfall Data (1992–2022)	Erbil meteorological station
Sentinel 2A satellite image (10 m spatial resolution) (acquired on 27 March 2022)	Downloaded from U.S Geologic Survey (http:// earth explo rer. usgs. gov/)
River map of the study area with 15 arc-second resolutions	Downloaded from the HydroSHEDS website (https:// www. hydro sheds.org/)
Soil Map of the World at 1:5 000 000 scale	Downloaded from the FAO/UNESCO Soil Map of the World(http://www.fao.org/soils-portal/soil-survey/soil-maps-and-databases/faounesco-soil-map-of-the-world/en/)
Hydrologic Curve Number of the study area	Downloaded from the Hydrologic Curve Number website (https://jaafarhadi.users.earthengine.app/view/hydrologic-curve-number#GEE)

Methods

The (AHP) and GIS-based multi-criteria decision-making are integrated to map and identify possible flood-prone locations in the area of interest. Eleven factors, elevation (El), land slope (Sl), flow accumulation (FA), rainfall (Rf), distance to rivers (DR), drainage density (DD), net runoff (NR), land use land cover (LULC), groundwater depth (GD), Normalized Difference Vegetation Index (NDVI) and soil type (ST) that influence the likelihood of floods were all mapped out in raster form using remote sensing and GIS techniques (Fig. 4).

Using the reclassify and resample tools that are available in spatial analysis and data management tools within ArcGIS environment, all raster factor maps are reclassified into a 10-meter spatial resolution measurement scale that ranged from one (very low) to five (very high). Immediately following reclassification for all flood-controlling factor maps, the AHP method is utilized to determine the degree to which each element contributed to the disaster. To develop the district's final flood susceptibility map, eleven flood-controlling spatial layers are placed in ArcGIS environment using the weighted overlay approach. To do an AHP analysis, in addition to processing, creating, and overlaying digital raster layers, respectively. It is necessary to make full use of ArcGIS 10.4, ERDAS Image 2014, and Microsoft Excel.

Methods of flood-controlling factor mapping techniques and reclassification

There's neither set list of factors that must be taken into account when utilizing multi-criteria decision-making to map flood susceptibility, nor a standard method for choosing factors. Eleven criteria that are closely related to flood occurrence are chosen for this research based on the evaluation of prior research, the availability of data, expert opinion, and the physical and research area's natural configuration. Factors included for this research and methods are used to analyze and create as described below. An elevation factor map has been created by rearranging the district's digital elevation model map into 5 flood susceptibility classes and scaling it to a 10-meter spatial resolution. A DEM is a continuous surface represented as a raster image, where each cell represents an elevation of a certain location. Slope maps are produced directly from DEM map of the research region using slope tools in spatial analyst tools of ArcGIS environment. After the district's DEM map is filled in to provide a depression- and sink-free DEM, a flow direction is created.

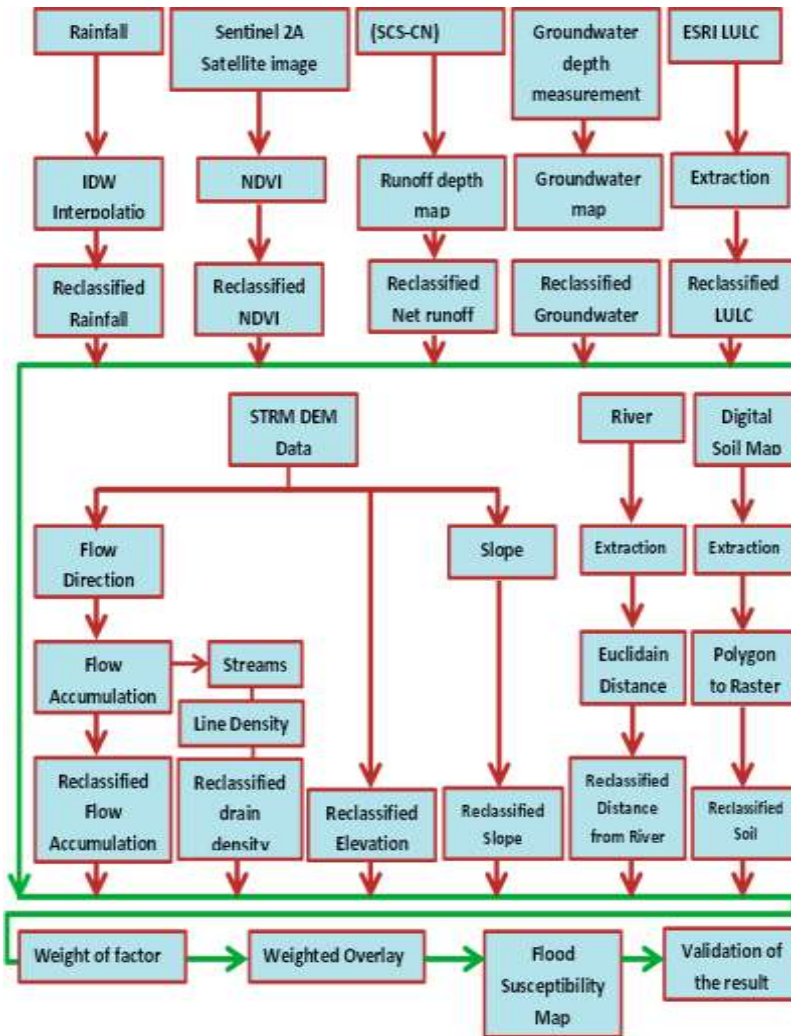


Fig. 4. Flowchart of the procedure for mapping and identification of flood-prone areas

A flow direction map is then used to construct a flow accumulation raster map. Hydrology tools like fill, flow direction, and flow accumulation, respectively, in spatial analyst tools in the ArcGIS program are used to fill DEM map, to create flow direction, and calculate flow accumulation. Next, the research area's continuous rainfall map will be created using the annual average. Using the ArcGIS raster calculator tool, a drainage network map is created based on the flow accumulation map. Then, using the drainage line processing in the spatial analyst tools, a drainage density map is made from the drainage network map. Distance to the river raster map is computed using the Euclidean distance tool. District's LULC map is first taken from the LULC map that is acquired from the ESRI website to create the LULC factor map. To create a soil type factor map, the Ministry of Water Resources and Agriculture's digital soil map of Iraq is accessed, and ArcGIS 10.4 software is used to extract soil types from watershed. The extracted vector soil map is then transformed into a raster format. Sentinel 2A satellite image retrieved from the US Geological Survey website is used to create the district's NDVI map. The SCS-CN model is used to estimate the annual net runoff volumes.

Analytical hierarchy process (AHP)

Multi-criteria decision-making to determine relative weight for each criterion or element are taken into consideration (AHP); first introduced by Saaty in 1987, is the most often applied and successful technique. Numerous prior studies have also employed this method (Aydin and Birincioğlu, 2022; Ajibade *et.al.*,2021; Astutik, *et.al.*,2021; Allafta and Opp, 2021; Das and Gupta, 2021; Karymbalis *et.al.*,2021; Mahmoud and Gan, 2018; Danumah *et.al.*,2016; Elsheikh *et.al.*,2015). To identify and map flood-prone areas, this

strategy was utilized by Ogato *et.al.* (2020) to assign weights to each flood control component. Based on an evaluation of earlier studies as well as the physical characteristics of the research location, weights were allocated to the variables utilized in multi-criteria decision-making process for mapping flood susceptibility. Proportional weights for every flood-controlling component used in this experiment are assigned according to Saaty (1987) (Table 2).

Table 2: The classifications, rating values, area coverage, and percentage of flood conditioning factors.

Factor	Class	Flood susceptibility	Rating	Class pixels	Area	
					ha	Percent (%)
Elevation (El) (m)	229 – 371	Very high	5	7862569	78625.69	37.31%
	371 – 476	High	4	7750725	77507.25	36.78%
	476 – 618	Moderate	3	2950843	29508.43	14.00%
	618 – 789	Low	2	1829045	18290.45	8.68%
	789 – 1108	Very low	1	679632	6796.32	3.22%
Slope (Sl) (degree)	0 – 1.28	Very high	5	6041961	60419.61	28.67%
	1.28 – 4.48	High	4	1077970	107797.1	51.15%
	4.48 – 8.48	Moderate	3	2920528	29205.28	13.86%
	8.48 – 14.40	Low	2	1021196	10211.96	4.85%
	14.40 – 40.80	Very low	1	309424	3094.24	1.47%
Flow Accumulation (FA) (pixels)	0 - 250,000	Very low	1	2103514	210351.4	99.82%
	250,000 - 1,000,000	Low	2	25335	253.35	0.12%
	1,000,000 - 2,250,000	Moderate	3	7830	78.3	0.037%
	2,250,000 - 4,250,000	High	4	2912	29.12	0.014%
	4,250,000 - 6,874,437	Very high	5	1596	15.96	0.008%
Rainfall (Rf) (mm)	280 – 348	Very low	1	16189	161.89	33.68%
	348 – 416	Low	2	11702	117.02	24.35%
	416 – 495	Moderate	3	8309	83.09	17.29%
	495 – 581	High	4	7118	71.18	14.81%
	581 – 732	Very high	5	4748	47.48	9.88%
Distance to the rivers (DR) (m)	0 – 500	Very high	5	1154398	11543.98	49.30267
	500 – 1000	High	4	733491	7334.91	31.32634
	1000 – 1500	Moderate	3	451764	4517.64	19.29419
	1500 – 2000	Low	2	1732	17.32	0.073971
	2000 – 2500	Very low	1	66	0.66	0.002819
Drainage density (DD) (km/km ²)	0 – 118	Very low	1	9438	94.38	19.63550
	118 – 236	Low	2	22416	224.16	46.63587
	236 – 354	Moderate	3	13392	133.92	27.86169
	354 – 472	High	4	2534	25.34	5.271918
	472 – 590	Very high	5	286	2.86	0.595015
Net runoff (NR) (mm)	270 - 286	Very low	1	14236	142.36	29.62%
	286 - 290	Low	2	19954	199.54	41.51%
	290 - 295	Moderate	3	4684	46.84	9.75%
	295 - 304	High	4	4449	44.49	9.26%
	304 - 320	Very high	5	4743	47.43	9.87%
Land use/Land cover (LULC)	Dense vegetation	Very low	1	4659	46.59	0.022%
	Trees	Low	2	532	5.32	0.003%
	Rangeland	Moderate	3	1135528	113552.8	53.88%
	Crops and Bare ground	High	4	4644349	46443.49	22.04%
	Built area and Water body	Very high	5	5067992	50679.92	24.05%
Groundwater depth (GD) (m)	200 - 287	Very high	5	18291	182.91	38.05%
	287 - 380	High	4	15275	152.75	31.78%
	380 - 520	Moderate	3	7853	78.53	16.34%
	520 - 708	Low	2	4739	47.39	9.86%
	708 - 962	Very low	1	1908	19.08	3.97%
Normalized Difference Vegetation Index (NDVI)	0 - 0.336	Very high	5	821072	8210.72	35.07%
	0.336 - 0.632	High	4	689086	6890.86	29.43%
	0.632 - 0.975	Moderate	3	402350	4023.5	17.18%
	0.975 - 1.378	Low	2	280543	2805.43	11.98%
	1.378 - 2.668	Very low	1	148399	1483.99	6.34%
Soil Type (ST)	Calcaric Fluvisols	Moderate	3	35	0.35	0.07%
	Calcic Xerosols	High	4	10317	103.17	21.55%
	Chromic Vertisols	Very high	5	37509	375.09	78.37%

Flood susceptibility map preparation approach

The flood susceptibility map of the area of interest is created by combining and overlaying spatial layers using weighted overlay technique, which is available in spatial analyst extension of ArcGIS environment. Following preparation and reclassification for each flood-control element using ArcGIS software to a standard measurement scale ranging from one (very low) to five (very high), as well as weighting of components using AHP approach, this result is achieved. Several earlier works including Aydin and Birincioğlu (2022), Allafta and Opp (2021), Das and Gupta (2021), Ali et.al. (2020), Dash, and Sar, (2020), Hadipour et.al. (2020), and Kanani, et.al. (2019) have utilized this equation (Eq. 1) in order to construct flood vulnerability maps.

$$FS = \sum_{i=0}^n x_i * w_i \dots\dots\dots (1)$$

Where *FS* is the criterion for flood susceptibility, x_i is the specific normalized criterion, *n* is number of criteria, and w_i is criterion's individual weight. The raster map of flood susceptibility output is produced by multiplying cell/pixel values of raster layers by the weight or percentage influence determined by the AHP analysis.

Results and discussion

Flood controlling factors processing

In the area of interest, eleven different flood-control factors are utilized. Elevation (El), land slope (Sl), flow accumulation (FA), rainfall (Rf), distance to rivers (DR), drainage density (DD), net runoff (NR), land use land cover (LULC), groundwater depth (GD), Normalized Difference Vegetation Index (NDVI) and soil type (ST) are some of the factors utilized to locate and map potential flood-prone that are susceptible to flood inundation. The spatial distribution of flood susceptibility in the research region is found and mapped through the process of investigating and analyzing these components. Following is a presentation of more information regarding the analysis of each factor.

Elevation

Elevation is one of the criteria that is taken into consideration when calculating the likelihood of floods occurring. Because they have a relatively larger river discharge and flood more quickly during high water, lower elevated regions are often more likely to experience floods than higher elevated places (Lee and Rezaie, 2022; Hong *et.al.*,2018a, b; Zzaman *et.al.*,2021). This is because lower elevated regions have a higher river discharge. The elevation of the region under investigation ranges from 206 to 1076 m above mean sea level.

The study area's low-elevation regions in the south and southwest (altitudes below 500 m a.s.l) are the most susceptible to flooding as Figure 5a illustrates. Conversely, the central regions of the district, which span from southeast to northwest and have an elevation exceeding 500 m a.s.l, are very susceptible to flooding. A significant portion of the research area, roughly 37.31% and 36.78%, is susceptible to flooding and inundation, correspondingly (Table 2).

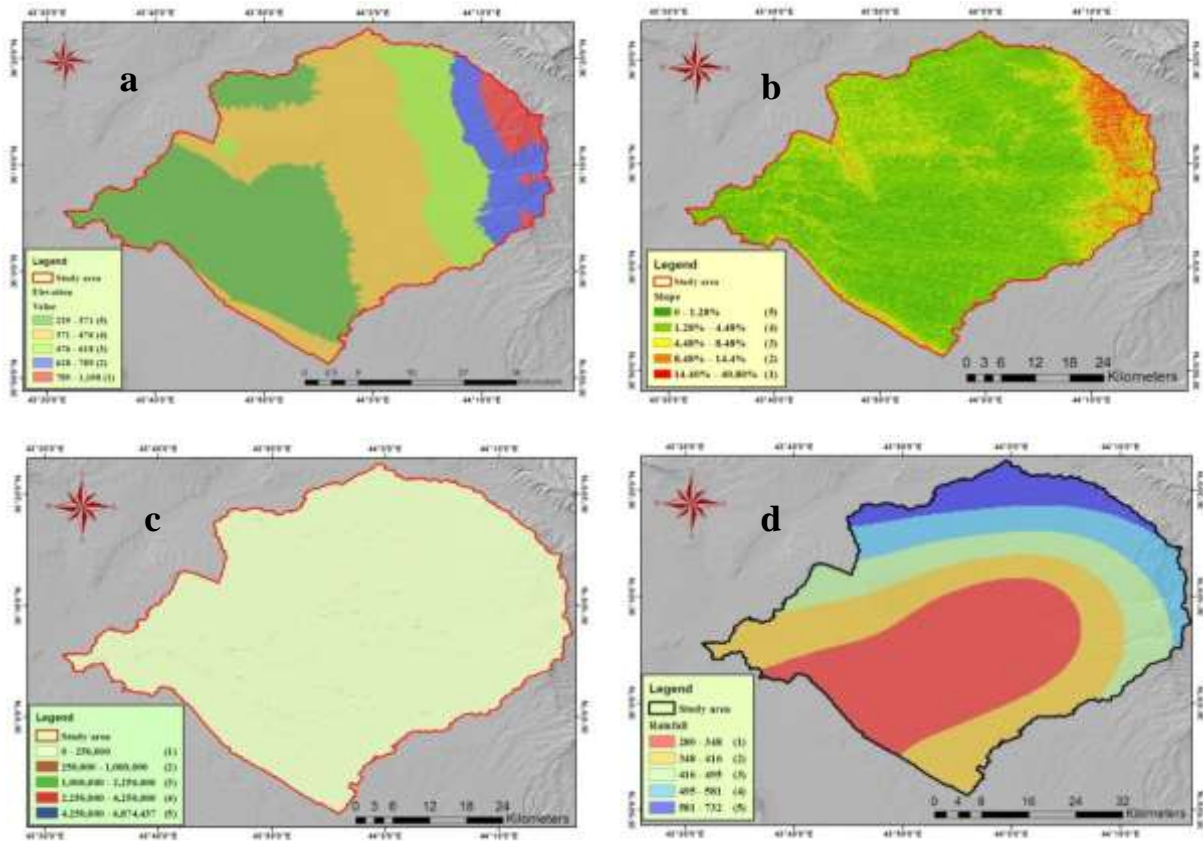


Fig. 5. Maps of the elevation (a), slope (b), flow accumulation (c), and rainfall factors (d).

Slope

The terrain's slope controls the flow rate of surface water. Volume of water covering land increases along with likelihood of a flood as slope falls (Das and Gupta, 2021; Astutik *et.al.* 2021; Zzaman *et.al.*,2021). Floods are more common in lowlands and flatlands with gentle slopes than in mountainous areas, which frequently have steeper slopes that prevent water from collecting (Wang *et.al.*, 2015). Based on reclassified slope map (Fig. 5b), the research area's very high sensitivity to flood inundation is represented by approximately 28.67% of slopes ranging from 0 to 1.28 degrees, high (1.28°–4.48°), and moderate (4.48°–8.48°) susceptibilities to floods, respectively, are found in about 51.15% and 13.86%, respectively. About 4.85% and 1.47%, respectively, are covered by areas with low (8.48–14.40°) and very low (14.40–40.80°) flood vulnerability (Table 2).

Flow accumulation

According to Ajibade *et.al.* (2021), flow accumulation is a method that visually represents the quantity of flow accumulated in each raster pixel. This flow accumulation is determined by the cumulative weights of the pixels that come before it. In accordance with the findings of Kazakis *et.al.* (2015), the accumulation of flow is most likely the most important element in determining the places that are susceptible to flooding. Through the utilization of flow accumulation, it can be able to create a map of the zone where surface runoff converges. The researchers conducted by Kazakis *et.al.* (2015) and Mahmoud and Gan (2018) indicate that a location that experiences a significant flow buildup is more likely to experience floods. Within the scope of this investigation, a reclassification strategy is utilized to segregate the flow accumulation of the research area into five distinct categories; very low, low, moderate, high, and very high flow accumulation values, which are used to classify flow accumulation values, as demonstrated in Figure (5c) and Table (2) respectively. Greater flow

accumulation values in a region, a greater likelihood that the region will be affected by flooding.

Rainfall

Because it is impossible to conceive of a flood occurring in the absence of rainfall, this factor needs to be taken into consideration while analyzing the vulnerability to floods. Flood inundation is the major component that causes floods to occur (Allafta and Opp, 2021). This is due to the fact that flood inundation is the outcome of a substantial amount of extremely heavy rainfall or prolonged rainfall (Hong *et.al.*, 2018aaand 2018b). Average annual rainfall in the district ranges from 280 to 732 mm, and the following new classifications have been implemented: very low, low, moderate, high, and very high contribution to flooding: 280–348 mm, 348–416 mm, 416–495 mm, 495–581 mm, and 581–732 mm, respectively. The categorization technique given by Das and Gupta (2021) is utilized in order to reclassify rainfall map for the research area. It is clear from Figure (5d) that the western parts of the research area are more susceptible to floods than eastern parts. According to Table (2), the percentages of the research regions are characterized as having a vulnerability to floods of very low, low, moderate, high, and very high.

Distance from the river

As a result of the fact that the excess water from rivers first reaches the river banks and the lowland areas that surround them, which are located in close proximity to rivers are more likely to experience flooding than regions that are located further away from rivers (Mahmoud and Gan, 2018). Because of this, height and slope will grow with distance (Lee and Rezaie, 2022; Zzaman *et.al.*, 2021) and to get desired effect. The research region is classed as having a high, moderate, low, and very low susceptibility to flooding respectively, for locations that are more than 2000 m away from the river. This classification is based on the distance as measured from the river. In contrast, areas that are less than 500 m away from river are categorized as having a very high sensitivity to flooding (Fig. 6a and Table 2). This is because these areas are geographically close to the river.

Drainage density

Drainage density is defined as the ratio of the total length of streams in an area to its total area, as stated by Zzaman *et.al.* (2021). According to Lee and Rezaie (2022); Das and Gupta (2021); Abdelkarim, *et.al.* (2020), and Mahmoud and Gan (2018), the drainage density of systems increases the likelihood of flooding. Additionally, an increase in surface runoff is brought about by drainage density. Similarly, drainage density value in this research is divided into 5 groups, as shown in Figure (6b) and Table (2): 0 - 0.4 km/km², 0.4 - 1 km/km², 1 - 1.5 km/km², 1.5 - 2 km/km², and > 2.1 km/km². These five groups represent the extremes of low and high levels, respectively. When looking at Figure (6b), the areas that have moderate drainage densities are depicted as light blue, whereas locations that have extremely high drainage densities are depicted as dark blue.

Net runoff (NR)

A model known as SCS-CN is utilized in order to find an estimate the annual net runoff volume. In order to estimate depth of surface runoff and then its volume for water that is obtained from a rainstorm, the model is a representation of the hypothesis that was developed by American Soil Conservation Service. The curve number is a number that indicates the extent to which the soil (land cover) absorbs precipitation water prior to the surface runoff process (USDA, 1986). This hypothesis takes into account the type of soil, land uses, land cover, and initial soil moisture. It then transforms these spatially variables into a number that is known as the curve number.

As can be seen in Figure (6c) and Table (2), the research area's net runoff (NR) is also classified into five distinct categories according to the degree to which it was prone to floods. These categories include very low, low, moderate, high, and very high, which in that order covered 29.62%, 41.51%, 9.75%, 9.26%, and 9.87% of the research area respectively.

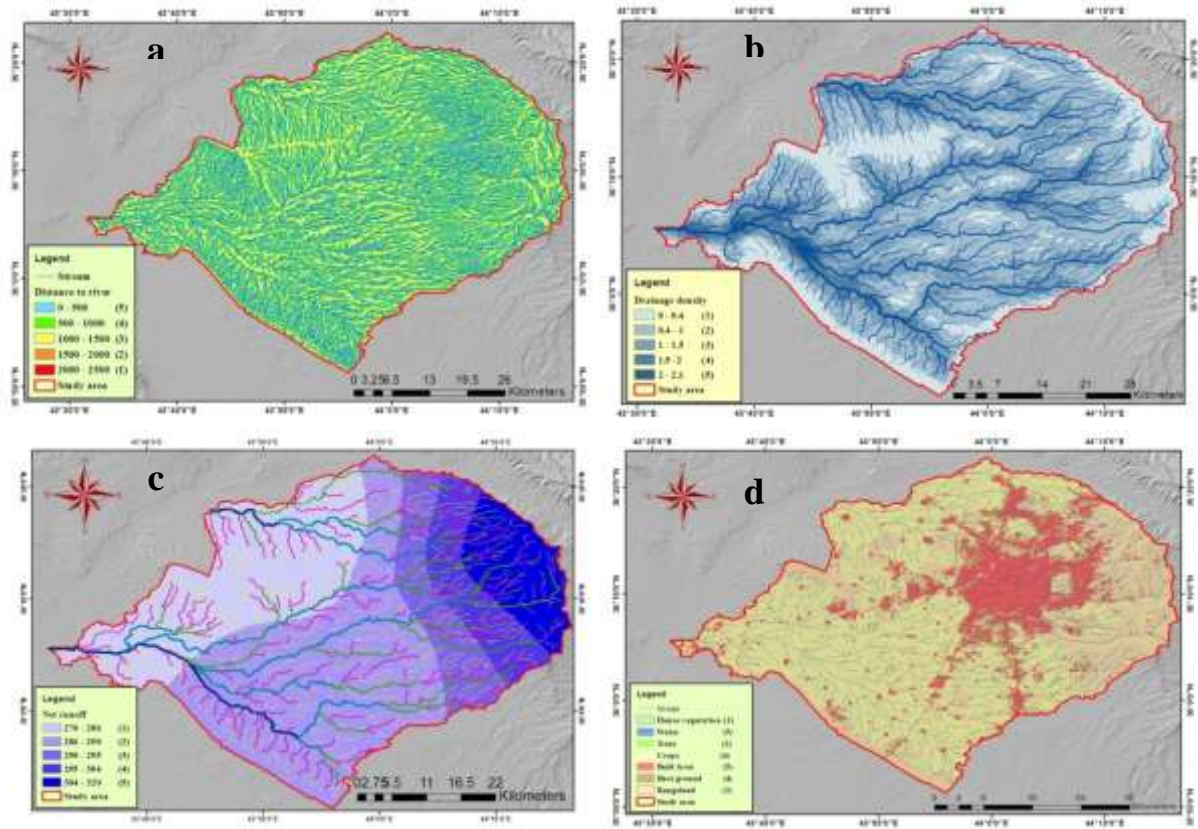


Fig. 6. Maps showing the distances to the rivers (a), drainage density (b), net runoff (c), and land use/cover (d) factors.

Land use and land cover (LULC)

There are several elements that play a significant role in determining the frequency of floods, including land use and land cover. Because dense vegetation slows down the rate at which water moves and increases the amount of water that can penetrate the soil, the areas that are covered by it are often less likely to be affected by flooding. Alternatively, surfaces those are impenetrable. On the other hand, runoff is shown to increase in residential and urban regions due to presence of impermeable surfaces and low infiltration (Allafta and Opp, 2021; Zzaman *et.al.*, 2021; Das and Gupta, 2021; Kazakis *et.al.*, 2015). Allafta and Opp. (2021) ranked the sensitivity of different types of land to floods as follows: very low, low, moderate, high, and very high. Shrub land, farms, bare land, urban areas, and waterbodies are determined to have the highest sensitivity to floods. The vulnerability to floods is categorized by Das and Gupta (2021) as having very high, high, moderate, low, and very low levels. Water bodies, build up, agriculture, sparse vegetation, dense vegetation, moderate and low vegetation, and moderate and low vegetation were all included in this classification. In addition, Hagos *et.al.* (2022) classified areas that were built up, grassland, farming, forestland, and shrubland as having varied degrees of sensitivity to floods. These degrees were as follows: very high, high, moderate, low, and very low. Similar to the previous example, the LULC map of the study region (shown in Fig. 6d and Table 2) reveals that susceptibility of area to floods are classified into five distinct categories: very high, high, moderate, low, and very low. Agriculture is the most important kind of land use and land cover (LULC) in the region, and it accounts for 53.88 percent of the research area (Fig. 6d and Table 2) with a significant risk of floods.

Analytical hierarchy process (AHP) analysis

An AHP analysis is performed after each flood-controlling part reclassification (Fig. 8). The purpose of this analysis is to determine the degree of importance or influence that each flood-controlling part possessed, which would then be implemented using a weighted overlay. Following the measures that Saaty (1987) said they should do is the creation of a matrix consisting of paired comparisons, the normalization of the pairwise comparison is computed, in addition to the weights of the factors, and the consistency of the comparison is examined with respect to the estimated influence that each component has on likelihood of flooding occurring in area under investigation. The flood-control elements' final criterion weight is as: elevation (17.61%), slope (15.16%), annual rainfall (11.36%), flow accumulation (14.86%), drainage density (8.13%), distance from rivers (11.04%), net runoff (5.69%), land use and land cover (7.21%), normalized difference vegetation index (2.82%), groundwater depth (3.97%), and soil type (2.15%).

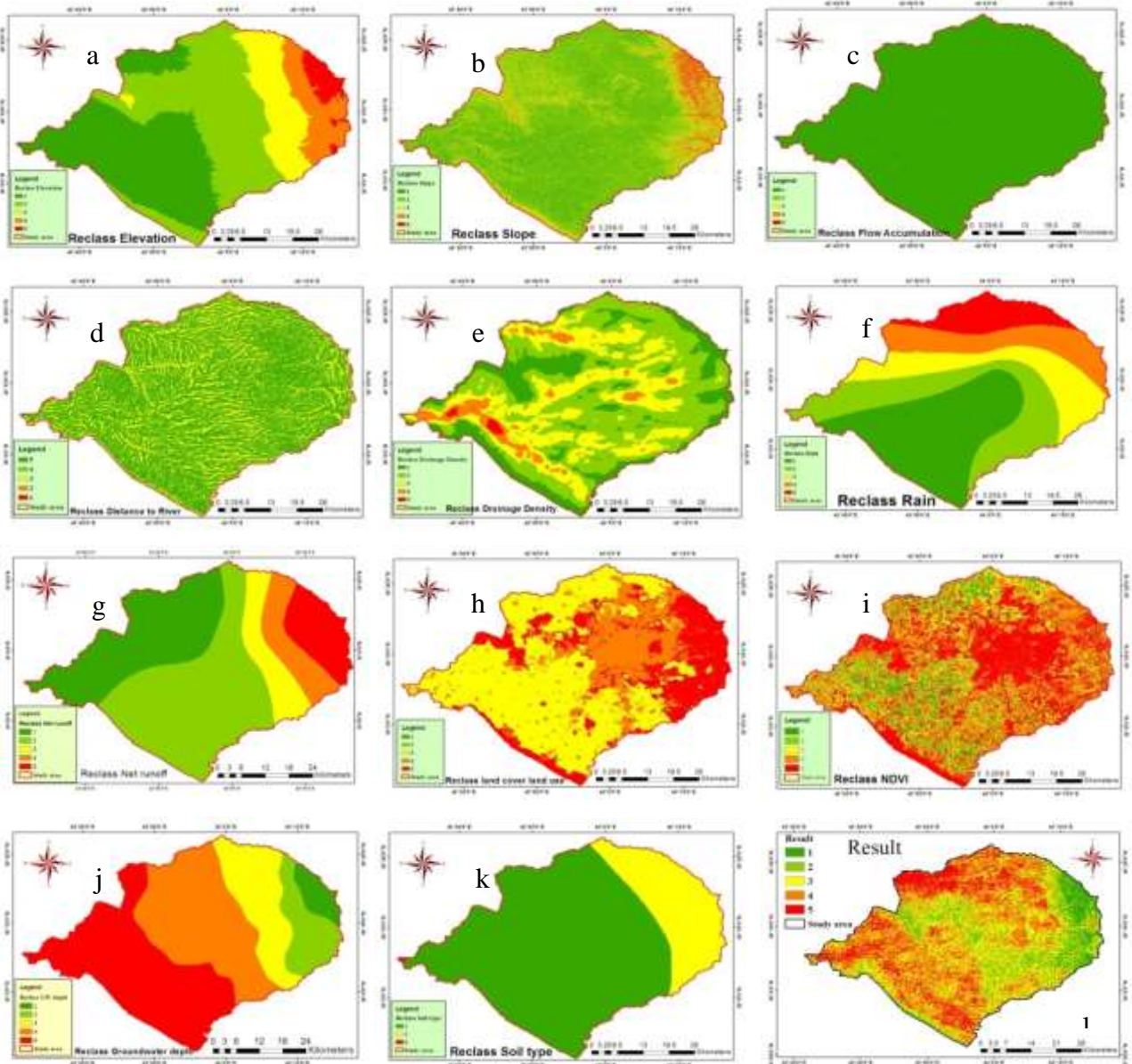


Fig. 8. Reclassification of flood-controlling factors (a-k) and result (l) map.

Flood susceptibility map of research area

The final flood susceptibility map for the sub-basin Erbil is illustrated in Figure (9), which is resulted by integrating eleven different thematic maps that were related to flood-

controlling variables. The district's flood susceptibility is classified using weighted overlay integration into five different classifications: very high, high, moderate, low, and very low. The area that is predicted to be associated with each susceptibility class is presented in Table (3). There is around 76.64% of total area that is susceptible to flooding, and this area has a moderate to very high vulnerability to flooding. The remaining 23.36 percent of the research region is characterized by a lack of flooding susceptibility that ranges from low to extremely low. According to flood susceptibility map (Fig. 9), the majority of research area's northern, northwestern, southern, and southwestern sections are considered to be the most vulnerable to flooding.

Table 3: Area coverage, percentage, and flood susceptibility

Flood susceptibility	Rating	Class pixels	Area	
			Hectares	Percent (%)
Very low	1	2968	29.68	6.18%
Low	2	8253	82.53	17.18%
moderate	3	14094	140.94	29.34%
High	4	15770	157.70	32.82%
Very high	5	6958	69.58	14.48%

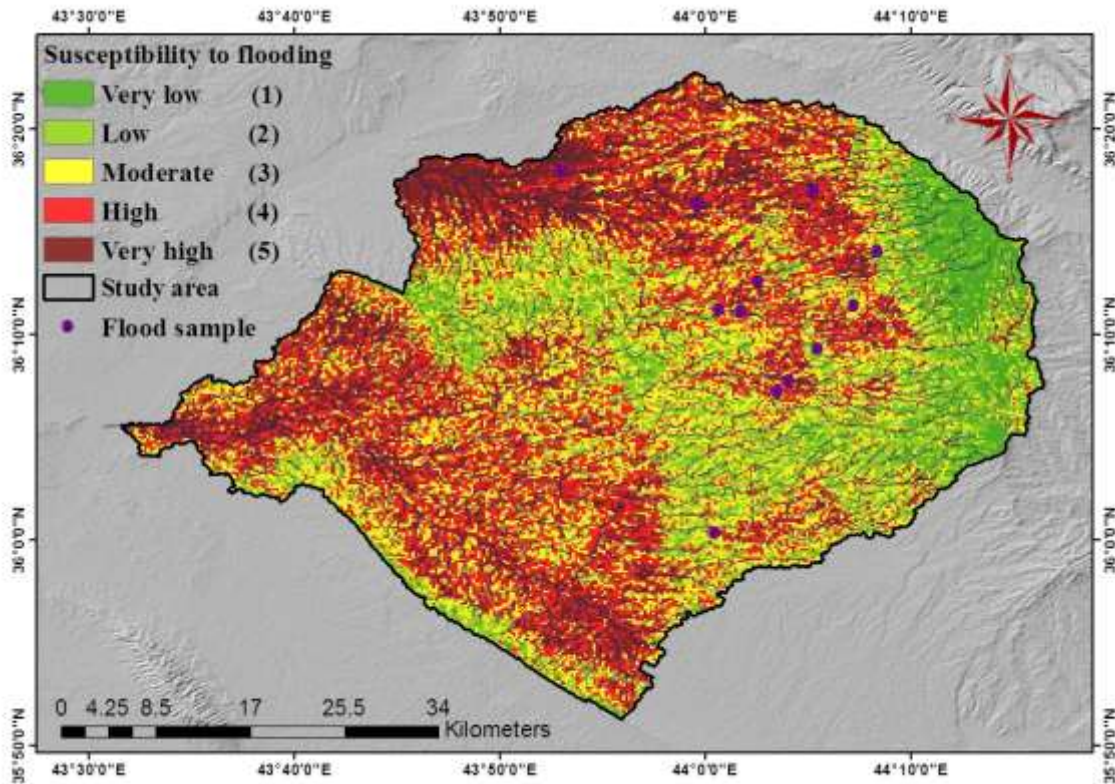


Fig. 9. Flood susceptibility map of research area

Flood susceptibility map of sub-basins

The model shows that 34.59% of Kasnazan sub-basin is very high to high degrees of the flood susceptibility, while the lowest severity is about 28.33%, very low to low degrees, but the moderate degree is about 37.07% in Kasnazan sub-basin as displayed in Table (4) and Figure (10a). The Daratwo sub-basin is located east of Erbil City, where it obtained an intensity score of 20.78% for very high to high degrees, while its minimum is about 48.31% for very low to low degrees. The moderate score is about 30.91% in the Daratwo sub-basin, as displayed in Figure (10b). The Qushtapa sub-basin is located south of Erbil City, where it obtained an intensity score of 34.97% for the very high to high degrees, while its minimum is about 31.31% for the very low to low degrees. The moderate score is about 33.71% in the Qushtapa sub-basin (Fig. 10c). The Grd Jotyar sub-basin is located north of Erbil City, where

it obtained an intensity score of 58.95% for the very high to high degrees, while its minimum is about 18.45% for the very low to low degrees. The moderate score is about 22.60% in the Grd Jotyar sub-basin (Fig. 10d). The Qoritan sub-basin is located south of Erbil City, with a severity score of 35.6% for very high to high degrees, while its minimum is about 28.29% for very low to low degrees. The moderate score is about 36.10% in the Qoritan sub-basin (Fig. 10e). The Darband sub-basin is considered the most dangerous in Erbil City, with a severity score of 72.59% for very high to high degrees, while the lowest severity is about 6.65% for very low to low degrees, but the moderate degree is about 20.76% in the Darband sub-basin, Fig. 10f. It is suggested that this methodology can be applied and adopted to draw a map of the risks of flash floods and circulate it anywhere in Iraq, especially in the western and southern regions, which are characterized by high rainstorms.

Table 4: Area coverage, percentage, and susceptibility to flooding in the sub-division basin

Sub-basins	Flood susceptibility	Rating	Class pixels	Area	
				ha	Percent (%)
Kasnazan	Very Low	1	328	3.28	5.03%
	Low	2	1519	15.19	23.30%
	Moderate	3	2416	24.16	37.07%
	High	4	1929	19.29	29.59%
	Very high	5	326	3.26	5.00%
Daratwo	Very Low	1	1552	15.52	19.46%
	Low	2	2301	23.01	28.85%
	Moderate	3	2465	24.65	30.91%
	High	4	1463	14.63	18.34%
	Very high	5	195	1.95	2.44%
Qushtapa	Very Low	1	290	2.90	6.91%
	Low	2	1024	10.24	24.40%
	Moderate	3	1415	14.15	33.71%
	High	4	1187	11.87	28.28%
	Very high	5	281	2.81	6.69%
Grd Jotyar	Very Low	1	401	4.01	6.64%
	Low	2	713	7.13	11.81%
	Moderate	3	1365	13.65	22.60%
	High	4	2132	21.32	35.30%
	Very high	5	1428	14.28	23.65%
Qoritan	Very Low	1	143	1.43	3.25%
	Low	2	1100	11.00	25.04%
	Moderate	3	1586	15.86	36.10%
	High	4	1302	13.02	29.64%
	Very high	5	262	2.62	5.96%
Darband	Very Low	1	34	0.34	1.23%
	Low	2	150	1.50	5.42%
	Moderate	3	575	5.75	20.76%
	High	4	1140	11.40	41.15%
	Very high	5	871	8.71	31.44%

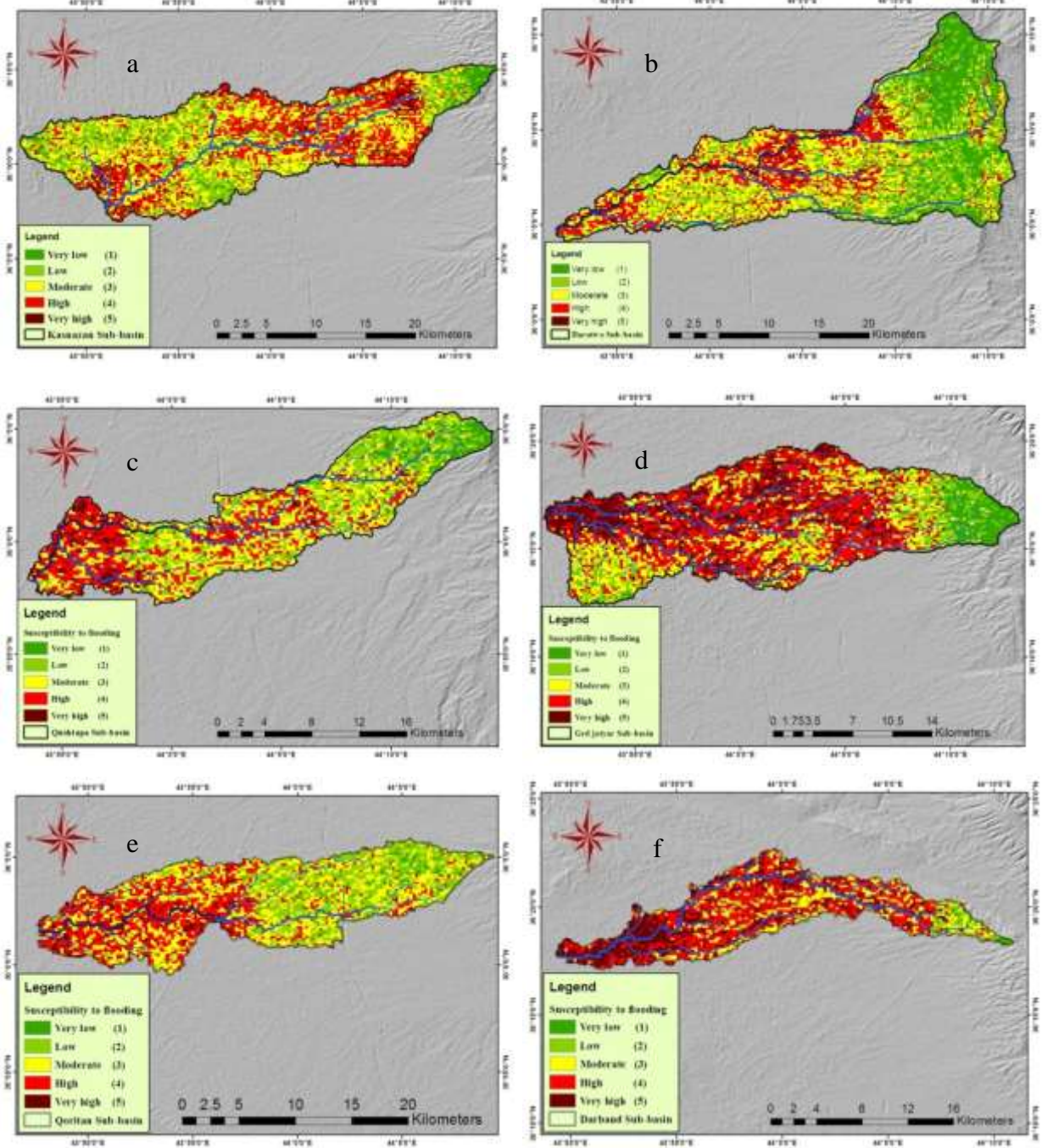


Fig. 10. Flash floods susceptibility map for the sub-division in the study area: Kasnazan Sub-basin (a), Daratwo Sub-basin (b), Qushtapa Sub-basin (c), Grd-Jotyar Sub-basin (d), Qoritan Sub-basin (e) and Darband Sub-basin (f).

Verification of the result

To ascertain whether or not the model's output truly depicts the conditions that exist in the field or on the ground, the model must be validated. The results of model can be compared to the actual flood event that was seen (Mahmoud and Gan, 2018; Ogato *et.al.*, 2020; Tadesse, et al., 2022; Hagos et al., 2022). This comparison can be made according to the findings of the model. Historical floods that have occurred in the research region are collected, and the positions of flood-prone places on the map created as a consequence of the research are compared. In addition, point data obtained from Google Earth is superimposed on flood susceptibility map that is generated by the model in order to verify the correctness of the model's output. Taking into consideration the recent floods and flash floods that have taken

place in Erbil, particularly the expulsion of Grd Jotyar, Daratwo, Qushtapa, Zeiren City, Korian City, Shekh Ahmad, Darband village, and Pirash village, the model of the study indicates that these locations are also among the most susceptible to the dangers of flooding. This means historical flood event in the region in which the flood occurred in the Grd Jotyar, Daratwo, Qushtapa, Zeiren City, Korian city, Shekh Ahmad, Darband village, and Pirash village demonstrated validity of flood vulnerability map that model predicted. It is also demonstrated that flood susceptibility map produced by the study's model is correlated well with the flood vulnerability map. It is also consistent with the findings of the study that this is the case in other areas that have been affected by flooding and flash floods in past. Over the course of this research period, this provides additional evidence that the output of the model may be relied upon.

Conclusion

Erbil's location and heavy rains make it one of the northern Iraqi cities most susceptible to flooding. This study has identified and mapped areas in the Erbil Basin that are vulnerable to floods using the integration of GIS, MCDM, and the AHP method. Eleven flood-control factors are calculated, mapped, weighted, and put on top of each other to find and map areas in the area of interest that might be prone to flooding. These factors include elevation, slope, flow accumulation, rainfall, distance to rivers, drainage density, net runoff, land use land cover, groundwater depth, Normalized Difference Vegetation Index and soil types. The findings indicate that the area of interest is very high, high, and moderate sensitivity to floods occurred in roughly 14.48%, 32.82%, and 29.34% of cases, respectively. Very low to low flooding susceptibility characterizes the remaining 23.36% of the area of interest. Areas with low elevation and generally flat slopes, high drainage densities, rainfall totals, flow accumulation, and crop land use and cover had the most risk of flooding. The Darband sub-basin, located in northern of Erbil, is rated as being the most hazardous in the Erbil City, with a severity score of 72.59% for very high to high degrees, 6.65% for very low to low degrees, and 20.76% for moderate degrees. The results show that the Daratwo sub-basin, which is located east of Erbil City, is less dangerous, as it obtained a severity score of 20.78% for the very high to high degrees, while the minimum is about 48.31% for the very low to low degrees. The moderate degree is about 30.91% in the Daratwo sub-basin. The sub-basins Grd Jotyar, Qoritan, Qushtapa, and Kasnazan have very high to high degrees of susceptibility to flooding, with 58.95%, 35.6%, 34.97%, and 34.59%, respectively. Validity of the model is assessed in this study by comparing its output to past flood episodes. Flood susceptibility maps of the model created are found to be in good accord with previous on-the-ground flood experiences. During the process of identifying and mapping flood-prone areas for purpose of effective flood risk management, it is discovered that the utilization of GIS-based MCDM and the AHP is not only effective but also less expensive.

References

- Abdelkarim, A., Al-Alola, S., Alogayell, H.M., Mohamed, S., Alkadi, I.I., Ismail, I., 2020. Integration of GIS-Based Multi-Criteria Decision Analysis and Analytic Hierarchy Process to Assess Flood Hazard on the Al-Shamal Train Pathway in Al-Qurayyat Region, Kingdom of Saudi Arabia. *Water*. <https://doi.org/10.3390/w12061702>.
- Ajibade, F., Ajibade, T., Idowu, T., Nwogwu, N.A., Adelodun, B., Lasisi, K., Opafola, O., Ajala, O., Fadugba, O., Adewumi, J., 2021. Flood - Prone Area Mapping Using GIS – Based Analytical Hierarchy Frameworks for Ibadan City, Nigeria. *Multi – Criteria decision analysis*. 28(5–6): pp. 283–295.

- Ali S., Parvin F., Pham Q., Vojtek M., Vojteková J., Costache R., Linh N., Nguyen H., Ahmad A., Ghorbani M., 2020. GIS – based comparative assessment of flood susceptibility mapping using hybrid multi - criteria decision – making approach, naïve Bayes tree, bivariate statistics and logistic regression: A case of Topľa basin, Slovakia. *Ecol Indic.* <https://doi.org/10.1016/j.ecolind.2020.106620>.
- Allafta H., Opp C., 2021. GIS-based multi-criteria analysis for flood prone areas mapping in the trans - boundary Shatt Al - Arab basin, Iraq - Iran. *Geomatic Nat Hazard Risk* 12(1):2087–2116. DOI: [10.1080/19475705.2021.1955755](https://doi.org/10.1080/19475705.2021.1955755)
- Astutik S., Pangastuti E., Nurdin E., Ikhsan F., Kurnianto F., Apriyanto B., Mujib M., 2021. Assessment of Flood Hazard Mapping Based on Analytical Hierarchy Process (AHP) and GIS: Application in Kencong District, Jember Regency, Indonesia. *Geosfera Indonesia.* <https://doi.org/10.19184/geosi.v6i3.21668>.
- Aydin M., Birincioğlu S., 2022. Flood risk analysis using gis-based analytical hierarchy process: a case study of Bitlis Province. *Applied Water Science.*
- Binns A., 2022. Sustainable development and flood risk management. *J Flood Risk Management.* <https://doi.org/10.1111/jfr3.12807>.
- Dang A., Kumar L., 2017. Application of remote sensing and GIS based hydrological modeling for flood risk analysis: a case study of District 8, Ho Chi Minh city, Vietnam. *Geomatic Nat Hazards Risk* 8(2):1792–1811. <https://doi.org/10.1080/19475705.2017.1388853>.
- Danumah J., Odai S., Saley BM., Szarzynski J., Thiel M., Kwaku A., Kouame F., Akpa L., 2016. Flood risk assessment and mapping in Abidjan district using multi – criteria analysis (AHP) model and geo information techniques. *Geo environment Disasters.* DOI: [10.1186/s40677-016-0044-y](https://doi.org/10.1186/s40677-016-0044-y)
- Das S., Gupta A., 2021. Multi - criteria decision based geospatial mapping of flood susceptibility and temporal hydro-geomorphic changes in the Subarnarekha basin, India. *Geoscience Front.* <https://doi.org/10.1016/j.gsf.2021.101206>.
- Dash P., Sar J., (2020); Identification and validation of potential flood hazard area using GIS-based multi - criteria analysis and satellite data - derived water index. *J Flood Risk Management.* <https://doi.org/10.1111/jfr3.12620>.
- Demir V., Kisi O., (2016); Flood Hazard mapping by using geographic information system and hydraulic model: Mert river, Samsun, Turkey. *Advance Meteorology.* <https://doi.org/10.1155/2016/48910.15>.
- Elsheikh R., Ouerghi S., Elhag A., (2015); Flood risk map based on GIS, and multi criteria techniques (case study Terengganu Malaysia). *07 (04): 348 – 357.* <https://doi.org/10.4236/jgis.2015.74027>.
- Erena S., Worku H., De Paola F., (2018); Flood hazard mapping using FLO - 2D and local management strategies of Dire Dawa city, Ethiopia. *J Hydrology Reg Stud* 19:224–239. <https://doi.org/10.1016/j.ejrh.2018.09.005>.
- Farhadi H., Najafzadeh M., 2021. Flood risk mapping by remote sensing data and random forest technique. *Water.* DOI: [10.3390/w13213115](https://doi.org/10.3390/w13213115)
- Jassim, S. Z. and Goff, J. C., 2006. *Geology of Iraq.* Czech Republic: Dolin, Prague and Moravian Museum, Brno, 341P.
- Hadipour V., Vafaie F., Deilami K., 2020. Coastal flooding risk assessment using a GIS-based spatial multi - criteria decision analysis approach. *Water.* DOI: [10.3390/w12092379](https://doi.org/10.3390/w12092379)

- Hagos Y., Andualem T., Yibeltal M., Mengie M., 2022. Flood hazard assessment and mapping using GIS integrated with multi-criteria decision analysis in upper Awash River basin, Ethiopia. *Applied Water Science*. DOI: [10.1007/s13201-022-01674-8](https://doi.org/10.1007/s13201-022-01674-8)
- Hong H., Panahi M., Shirzadi A., Ma T., Liu J., Zhu A., Chen W., Kougiyas I., Kazakis N., 2018. Flood susceptibility assessment in Hengfeng area coupling adaptive neuro-fuzzy inference system with genetic algorithm and differential evolution. *Science Total Environ* 621:1124–1141.
- Hong H, Tsangaratos P., Ilija I., Liu J., Zhu A., Chen W., 2018. Application of fuzzy weight of evidence and data mining techniques in construction of flood susceptibility map of Poyang County, China. *Science Total Environ* 625: 575 – 588. DOI: [10.1016/j.scitotenv.2017.12.256](https://doi.org/10.1016/j.scitotenv.2017.12.256)
- Kanani-Sadat Y., Arabsheibani R., Karimipour F., Nasserli M., 2019. A new approach to flood susceptibility assessment in data-scarce and ungauged region based on GIS-based hybrid multi – criteria decision - making method. *J Hydrology* 572: 17 – 31. <https://doi.org/10.1016/j.jhydrol.2019.02.034>.
- Karymbalis E., Andreou M., Batzakis D., Tsanakas K., Karalis S., 2021. Integration of GIS-based multi - criteria decision analysis and analytic hierarchy process for flood - hazard assessment in the Megalo Rema River Catchment (East Attica, Greece) Sustainability. <https://doi.org/10.3390/su131810232>.
- Kazakis N., Kougiyas I., Patsialis T., 2015. Assessment of flood hazard areas at a regional scale using an index – based approach and Analytical Hierarchy Process: application in Rhodope - Evros region, Greece. *Science Total Environ* 538: 555 – 563. DOI: [10.1016/j.scitotenv.2015.08.055](https://doi.org/10.1016/j.scitotenv.2015.08.055)
- Khoshnaw, N. J., 2022. Hydrogeological Investigation of the central part (central sub-basin) of the Erbil basin (North of Iraq), MA Thesis- Firat University, Graduate School of Natural and Applied Sciences, Turkey.
- Lee S., Rezaie F., 2022. Data used for GIS – based flood susceptibility mapping. *Data Geology. Ecological Ocean org. Space Science. Polar Science* 1:1-15.
- Mahmoud S., Gan T., 2018. Multi - criteria approach to develop flood susceptibility maps in arid regions of Middle East. *J Clean Prod* 196: 216 - 229.
- Ogato G., Bantider A., Abebe K., Geneletti D., 2020. Geographic information system (GIS)-Based multi – criteria analysis of flooding hazard and risk in Ambo Town and its watershed, West shoa zone, oromia regional State, Ethiopia. *J Hydrology Reg Stud*. <https://doi.org/10.1016/j.ejrh.2019.100659>.
- Ozkan S., Tarhan C., 2016. Detection of flood hazard in Urban areas using GIS: Izmir Case. *Procedia Technology* 22:373–381. DOI: [10.1016/j.protcy.2016.01.026](https://doi.org/10.1016/j.protcy.2016.01.026)
- Rahmati O., Zeinivand H., Besharat M., 2015. Flood hazard zoning in Yasooj region, Iran, using GIS and multi - criteria decision analysis. *Geomatic Nat Hazard Risk* 7(3):1000–1017. DOI: [10.1080/19475705.2015.1045043](https://doi.org/10.1080/19475705.2015.1045043)
- Razavi-Termeh S., Kornejady A., Pourghasemi H., Keesstra S., 2018. Flood susceptibility mapping using novel ensembles of adaptive neuro - fuzzy inference system and meta - heuristic algorithms. *Science Total Environ* 615:438–451. DOI: [10.1016/j.scitotenv.2017.09.262](https://doi.org/10.1016/j.scitotenv.2017.09.262)
- Saaty W., 1987. The analytic hierarchy process, what and how it is used. *Math Modell* 9(3-5):161-176

- Son N., Trang N., Bui X., Thi C., 2021. Remote sensing and GIS for urbanization and flood risk assessment in Phnom Penh, Cambodia. *Geocarto Int.* DOI: [10.1080/10106049.2021.1941307](https://doi.org/10.1080/10106049.2021.1941307)
- Tadesse D., Suryabhadgavan K., Nedaw D., Hailu B., 2022. A model-based flood hazard mapping in Itang District of the Gambella region, Ethiopia. *Geol Ecol Landsc.* DOI: [10.1080/24749508.2021.2022833](https://doi.org/10.1080/24749508.2021.2022833)
- Tamiru H., Dinka M., 2021. Artificial intelligence in geospatial analysis for flood vulnerability assessment: a case of dire Dawa Watershed, A wash Basin, Ethiopia. *Science World J* 2021:6128609. DOI: [10.1155/2021/6128609](https://doi.org/10.1155/2021/6128609)
- Tehrany M., Shabani F., Jebur M., Hong H., Chen W., Xie X., 2017. GIS - based spatial prediction of flood prone areas using standalone frequency ratio, logistic regression, weight of evidence and their ensemble techniques. *Geomatic Nat Hazard Risk* 8(2):1538–1561. DOI: [10.1080/19475705.2017.1362038](https://doi.org/10.1080/19475705.2017.1362038)
- Thannoun, R.G. and Ismaeel, O.A., 2024. Flood Risk Vulnerability Detection based on the Developing Topographic Wetness Index Tool in Geographic Information System. In *IOP Conference Series: Earth and Environmental Science* (Vol. 1300, No. 1, p. 120 12). IOP Publishing. DOI: [10.1088/1755-1315/1300/1/012012](https://doi.org/10.1088/1755-1315/1300/1/012012)
- USDA-TR55, 1986. *Urban Hydrology for Small Watersheds*, Department of Agriculture, USA.
- Wang Z., Lai C., Chen X., Yang B., Zhao S., Bai X., 2015. Flood hazard risk assessment model based on random forest. *Journal Hydrology* 527: 1130 – 1141. <https://doi.org/10.1016/j.jhydrol.2015.06.008>
- Wubalem A., Tesfaw G., Dawit Z., Getahun B., Mekuria T., Jothimani M., 2021. Comparison of statistical and analytical hierarchy process methods on flood susceptibility mapping: In a case study of the Lake Tana sub - basin in northwestern Ethiopia. *Open Geoscience* 13(1):1668–1688. DOI: [10.1515/geo-2020-0329](https://doi.org/10.1515/geo-2020-0329)
- Yariyan P., Avand M., Abbaspour R., Torabi A., Costache R., Ghorbanzadeh O., Janizadeh S., Blaschke T., 2020. Flood susceptibility mapping using an improved analytic network process with statistical models. *Geomatic Nat Hazard Risk* 11(1):2282–2314. DOI: [10.1080/19475705.2020.1836036](https://doi.org/10.1080/19475705.2020.1836036)
- Zhao G., Pang B., Xu Z., Yue J., Tu T., 2018. Mapping flood susceptibility in mountainous areas on a national scale in China. *Science Total Environ* 615: 1133 – 1142. DOI: [10.1016/j.scitotenv.2017.10.037](https://doi.org/10.1016/j.scitotenv.2017.10.037)
- Zzaman R., Nowreen S., Billah M., Islam A., 2021. Flood hazard mapping of Sangu River basin in Bangladesh using multi-criteria analysis of hydro geomorphological factors. *J Flood Risk Management*. DOI: [10.1111/jfr3.12715](https://doi.org/10.1111/jfr3.12715)